Peroxynitric Acid Decay Mechanisms and Kinetics at Low pH

Jean-Michel Régimbal[†] and Michael Mozurkewich*

Chemistry Department and Centre for Atmospheric Chemistry, York University, 4700 Keele Street, North York, ON, M3J 1P3 Canada

Received: June 11, 1997; In Final Form: August 26, 1997[⊗]

An efficient spectroiodometric method is described for the quantification of peroxynitric acid, $HOONO_2$, and H_2O_2 in dilute solutions. $HOONO_2$ reacts with I^- in acidic media with a rate constant of 1200 ± 300 M^{-1} s^{-1}. At 22 °C and pH 1.7, in the presence of 1.00 mM Na_2EDTA, the average lifetime for $HOONO_2$ thermal decay was found to be 49 ± 26 min, longer than reported in previous work. The addition of Na_2EDTA produced longer lifetimes, the longest one observed being 73.9 ± 0.9 min. Cu^{2+} was found to catalyze $HOONO_2$ decomposition. In the presence of large concentrations of $CuSO_4$, the decomposition rate is independent of $CuSO_4$ and is controlled by the rate of the dissociation reaction: $HOONO_2 \rightarrow HO_2 + NO_2$. For this reaction, we found a rate constant of $(5.27 \pm 0.15) \times 10^{17}$ s^{-1} $\exp(-110.1 \pm 1.3$ kJ $mol^{-1}/RT)$ from 5.0 to 25.0 °C and an equilibrium constant of $(1.5 \pm 0.2) \times 10^{-11}$ M at 25 °C, with an estimated reaction enthalpy of 87 ± 3 kJ mol^{-1}. With the use of auxiliary thermodynamic data, we find that the standard heat of formation of $HOONO_2$(aq) at 25 °C is -111 ± 2 kJ mol^{-1} and that the standard free energy of formation is 5.5 ± 1.5 kJ mol^{-1}. The Henry's Law constant is 12600 ± 4700 M atm^{-1}, with an enthalpy of solution of -57.1 ± 1.5 kJ mol^{-1}. The decomposition of $HOONO_2$ is base-catalyzed; between 5.0 and 25.0 °C the decay rate constant is $(1.16 \pm 0.20) \times 10^{16}$ M s^{-1} $[H^+]^{-1}$ $\exp(-126 \pm 8$ kJ $mol^{-1}/RT)$.

Introduction

Peroxynitric acid is a powerful oxidant that is formed in the atmosphere by the combination of HO_2 and NO_2 radicals.[1] Although it is present in the troposphere only at very low concentrations, it is continually being formed and is potentially a significant oxidant in atmospheric droplets and particles. However, it is difficult to evaluate its importance since there is little quantitative data on the thermodynamics and kinetics of aqueous $HOONO_2$.

Kenley et al. reported that $HOONO_2$ decays in aqueous solution with O_2 as a product.[2] They found a lifetime of 11 min at 11 °C and pH 1.36 in 10^{-3} M solutions. Lammel et al. reported a longer lifetime of 17 min at 25 °C.[3] These groups suggested that the decay proceeds via a free-radical mechanism:

$$HOONO_2 \rightleftharpoons HO_2 + NO_2 \quad (1)$$

$$2HO_2 \rightarrow H_2O_2 + O_2 \quad (2)$$

$$2NO_2 + H_2O \rightarrow HNO_2 + H^+ + NO_3^- \quad (3)$$

Løgager and Sehested have measured a lifetime of 23 min at 298 K and pH 2 and argue that the decay proceeds via a direct reaction:[4]

$$HOONO_2 \rightarrow HNO_2 + O_2 \quad (4)$$

They also reported that the pK_a of $HOONO_2$ is 5.85. All of the prior works agree that the decomposition is strongly base-catalyzed.

Appelman and Gosztola have reported a novel synthesis of $HOONO_2$ and determined a low-pH lifetime of 43 min at 298 K.[5]

An understanding of the rate and mechanism of the thermal decay of $HOONO_2$ is a prerequisite to further studies of its aqueous-phase kinetics. Thus, one of the objectives of the present work is to resolve these conflicts over the actual mechanism and lifetime of this decay. In addition, we are able to use the kinetic data to derive thermochemical parameters for $HOONO_2$(aq); in particular, the solubility of $HOONO_2$(g) is critical to the evaluation of the possible role of this species in atmospheric particles. To pursue these studies, we have developed a new and efficient method to monitor $HOONO_2$ concentrations in dilute acidic solutions.

One possible role for $HOONO_2$ in atmospheric particles is as an oxidant for Cl^-. It has been known for some time that sea salt aerosol particles often have $[Cl^-]$:$[Na^+]$ ratios inferior to that of sea water. The most common explanation for this phenomenon, known as the chloride deficit, is acid displacement.[6] In this mechanism, acidification of these particles by H_2SO_4 and HNO_3 drives Cl^- out as relatively unreactive HCl. Another hypothesis is oxidation of chloride into volatile and photolabile species like HOCl or Cl_2.[7] If this occurs, it is of potentially great significance for the chemistry of the marine boundary layer since these compounds are easily photolyzed to form highly reactive Cl atoms. Recent measurements have revealed the presence of photolyzable chlorine in the marine boundary layer[8] and Cl atoms in the Arctic boundary layer.[9] The mechanism for Cl oxidation in the atmosphere is not understood.

Experimental Section

Material and Solutions. All experiments have been done with water that was first deionized and then distilled from $KMnO_4$ in an all-glass apparatus. KI, $NaNO_3$, $CuSO_4 \cdot 5H_2O$, NaOH, ammonium molybdate, 70% HNO_3, 85% H_3PO_4, 98% H_2SO_4, 30% H_2O_2, pH 4.00 phthalate buffer (all from BDH), glacial CH_3COOH (Caledon), Na_2EDTA, $ClCH_2COOH$ (both from Fisher Scientific), pH 2.00 HCl/KCl standard solution (VWR), and $NaNO_2$ (J. T. Baker) were used as supplied. Other

* Corresponding author. E-mail: mozurkew@yorku.ca.
[†] E-mail: jmr@yorku.ca.
[⊗] Abstract published in *Advance ACS Abstracts,* October 15, 1997.

S1089-5639(97)01908-7 CCC: $14.00

buffers were prepared from the appropriate acids and NaOH and were typically 0.10 M.

$HOONO_2$ Synthesis. $HOONO_2$ was prepared with a slightly scaled-up version of the synthesis described by Appelman and Gosztola,[5] but with $HClO_4$ replaced by 70% HNO_3. The resulting solution will be referred to as the reaction mixture. It was stored at about −18 °C and significant amounts of $HOONO_2$ remained after about three weeks. FT-Raman spectrophotometry gave a spectrum identical to the one previously reported.[5] Iodometric titrations gave average $HOONO_2$ and H_2O_2 concentrations of 1.6 and 2.4 M in the reaction mixture, respectively.

The reaction mixture was normally diluted by a factor of about 10^3 for measurements of reaction rates. We found that Na_2EDTA stabilizes $HOONO_2$ in this dilute reaction mixture, so we added 1.0 mM Na_2EDTA to it, unless otherwise stated. For the classical and kinetic spectroiodometry procedures, 70.0 μL of the reaction mixture were added to 50.00 mL of the appropriate HNO_3 or buffer solution. In a few instances, H_2SO_4 was used. In the flow experiments, 20.0−100 μL of reaction mixture were added to 50 mL of the appropriate HNO_3 or buffer solution.

Apparatus. For all experiments, a Hewlett-Packard 8452A diode-array UV−visible spectrophotometer was used, with a 1 cm path-length quartz cell. It can take simultaneous readings at 2 nm intervals in the 190−820 nm range, but, normally, only the 280−360 nm range was used. It was equipped with a HP Peltier temperature-controller 89090A that set the cell temperature to 25.0 °C and stirred the solution at 600 rpm with a small magnet cast in glass. Nothing showed that mixing could have been a rate-limiting step.

pH measurements were made with a pH meter (10 Accumet, Fisher Scientific), standardized at the appropriate temperatures with pH 4.00 (potassium phthalate, 0−25 °C) and pH 2.00 (0.05 M KCl/HCl, 25 °C) buffer solutions. We assumed the second buffer to have a pH value independent of temperature between 5.0 and 25.0 °C.

To control the temperature, a Neslab RTE-210 thermostated bath was used to circulate fluid through a 50 mL jacketed beaker equipped with a magnetic stirrer.

Spectroiodometry—Basic Principles. Kinetic studies have been done by measuring spectrophotometrically the triiodide produced by reactions 5−7. Reaction 6 requires an ammonium

$$HOONO_2 + 2I^- + H^+ \rightarrow H_2O + NO_3^- + I_2 \qquad (5)$$

$$H_2O_2 + 2I^- + 2H^+ \rightarrow 2H_2O + I_2 \qquad (6)$$

$$I_2 + I^- \rightleftharpoons I_3^- \qquad (7)$$

$$O_2 + 4I^- + 4H^+ \rightarrow 2I_2 + 2H_2O \qquad (8)$$

molybdate catalyst to go at an appreciable rate. Reaction 8 causes some interferences when the catalyst is present in solution.

In this procedure, part of the dilute reaction mixture is mixed with a large volume of KI solution. $HOONO_2$ reacts quickly with I^-, which is in large excess, and I_3^- becomes the dominant oxidized iodine species in solution ($K_7 = 720$).[10] At these low pH values, HOI and OI^- are negligible. I_3^- has large absorption coefficients at 288 (ϵ = 40 000 M^{-1} cm^{-1}) and 352 nm (ϵ = 26 400 M^{-1} cm^{-1});[11] this second peak was used to monitor the decay. The 288 nm one was rejected because the molybdate catalyst absorbs in that region. Under the conditions of our experiments, reactions 6 and 8 were almost negligible, unless catalyst was added to the KI solution. This allowed us to distinguish oxidation of I^- by $HOONO_2$ from oxidation by H_2O_2.

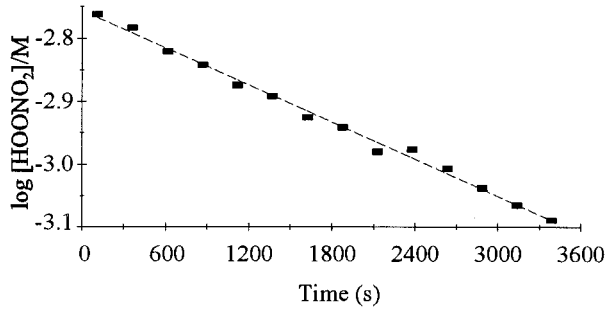

Figure 1. Typical $HOONO_2$ decay plot obtained from classical spectroiodometric data. Done with 0.019 M H_2SO_4 at room temperature and with 1.00 mM Na_2EDTA. Logarithms in base 10. Dashed line is linear regression of the data.

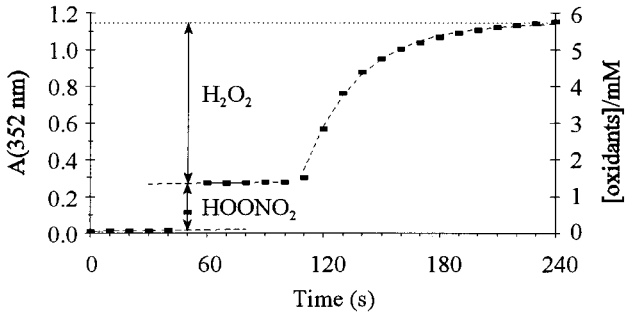

Figure 2. Typical time trace obtained for a classical spectroiodometric run. Dashed lines are fits of the data to linear (first two parts) or nonlinear models (last part); dotted line indicates A_∞.

Three different forms of spectroiodometry have been developed in the course of this work: classical, kinetic, and flow. The first one is ideal for $HOONO_2$ lifetimes of 20 min or more, the second one was used to measure the rate constant of the reaction between $HOONO_2$ and I^-, and the last one was used for short lifetimes (down to 20 s). $HOONO_2$ decay was always studied under first-order or pseudo-first-order conditions.

All the uncertainties based on our measurements are given in the text at the 95% confidence level determined from sample standard deviation. We assume that all the uncertainties found in the literature were also for this confidence level.

Classical Spectroiodometry. In classical spectroiodometry, 2.00 mL of 8.0 mM KI were pipetted into the UV absorption cell and acidified with 20.0 μL of 2.4 M HNO_3. Readings were taken every 10 s and lasted 1 s each. After 50 s, 20.0 μL of dilute reaction mixture was added to the stirred cell and reaction 5 caused a rapid increase in absorbance. 110 s after the start of the run, 20.0 μL of 2% ammonium molybdate solution was added to the cell and reactions 6 and 8 started producing significant amounts of I_3^-, reaction 6 being the dominant one. The total run length was 4 min. Usually, 10−14 consecutive samples from the same dilute reaction mixture were used to get a decay plot of $HOONO_2$, at least when it had a relatively long lifetime. Figure 1 is such a plot; for faster decays, it was not exceptional to rely on as little as four data points to find the lifetime.

Figure 2 shows a typical time trace of a classical spectroiodometric run. The $HOONO_2$ concentration is extracted by extrapolating the first and second regions to the dilute reaction mixture addition time to obtain the absorbance difference, ΔA, at this time. [$HOONO_2$] was then computed from eq I, where V_{cell} and $V_{aliquot}$ are the solution volumes in the cell (2.04 mL) and in the dilute reaction mixture aliquot (20.0 μL), respectively,

$$[\mathrm{HOONO_2}] = \frac{\Delta A}{\epsilon(\mathrm{I_3^-}, 352\ \mathrm{nm})b}\frac{V_{\mathrm{cell}}}{V_{\mathrm{aliquot}}}\left(\frac{1}{K_7[\mathrm{I^-}]}+1\right) \quad \text{(I)}$$

and the last term is a correction for free iodine in solution. Variation in the blank readings produced uncertainties of about 1×10^{-2} mM in $[HOONO_2]$.

The catalyzed portion of the curve was fit to eq II, using SigmaPlot (Marquardt−Levenberg algorithm); Figure 2 shows how well the fit matched the data. A_∞ is the absorbance at

$$A(t > t_{\mathrm{cat}}) = (A_\infty - A_{\mathrm{H_2O_2}}\, e^{-k_{cat}(t-t_{cat})}) + k_{\mathrm{O_2}}(t-t_{\mathrm{cat}}) \quad \text{(II)}$$

$t \rightarrow \infty$ in the absence of O_2 interference, $A_{H_2O_2}$ is the asymptotic increase in absorbance due to the catalyzed reaction 6, k_{cat} is the pseudo-first-order rate constant of reaction 6, t_{cat} is the catalyst addition time (i.e., 110 s), and k_{O_2} is the rate of production of I_3^- by reaction 8. In 361 runs, the latter ranged from 5.7 to 15.8 $\times 10^{-4}$ s^{-1}, with an average of (9.4 ± 2.8) $\times$ 10^{-4} s^{-1}. The uncertainty in individual mean H_2O_2 concentrations on any given set of runs was usually about 6 ± 3%.

Kinetic Spectroiodometry. This was used to measure the rate constant for reaction 5 to determine if it was fast enough to be used in flow experiments. Only a few details differed from classical spectroiodometry: the KI solution was only 80 μM, the runs lasted but 1 min with the dilute reaction mixture aliquot added after 10 s, readings were 0.4 s long and were taken every 2 s, and no catalyst was added. Because of the dilution of I^-, I_2 was the dominant form of oxidized iodine in solution and very little I_3^- could be detected. The time trace obtained was fit to eq III, to obtain k_5, the rate constant for reaction 5.

$$A(t>10\ \mathrm{s}) = A_\infty - A_{\mathrm{HOONO_2}}(1 - e^{k_5[\mathrm{I^-}](t-t_0)}) \quad \text{(III)}$$

In the pH range 1.8−4.2, the average value of k_5 was found to be 1200 ± 300 M^{-1} s^{-1}. Details of the kinetics of this reaction will be discussed in a future publication. Under the conditions used for classical and flow spectroiodometry, $HOONO_2$ had a typical lifetime of 0.10 s against reduction by I^-. Thus, this reaction may be taken as being fast compared to the other ones studied by these techniques.

Flow Spectroiodometry. A schematic of the flow system is shown in Figure 3. We used a Masterflex peristaltic pump model 7520-35 with Tygon tubing (i.d. 3.1 mm) for the eluent channel and Norprene tubing (i.d. 0.8 mm) for the sample channel. These were not themselves immersed in the solution but rather drew the solution through glass tubes. The two channels were connected to a Teflon PTFE tee by Kynar fittings; the tee was linked to a Hellma Suprasil flow cell (100 μL chamber volume) by a 50 cm long fluorinated ethylene−propylene copolymer (FEP) tube. Varying the pump speed during the study of a $HOONO_2$ decay at room temperature did not affect the results, indicating that there was no mixing problem in the system.

At the normal operating condition of 25 ± 2 rpm (16.8 ± 1.3 mL/min), it took about 10 s for the dilute reaction mixture to reach the tee and less than 1 s to travel from it to the cell; the residence time in the cell was about 0.4 s. The sample dilution ratio, α, was determined by drawing a $CuSO_4$ solution through the sample channel and measuring its concentration in the cell from its absorbance at 808 nm; the ratio of this concentration to that of the original solution gave α. Usually, α = 0.08−0.09. A comparable procedure with $NaNO_3$ in the eluent channel was used to determine the eluent dilution ratio (1 − α); the two were consistent with each other.

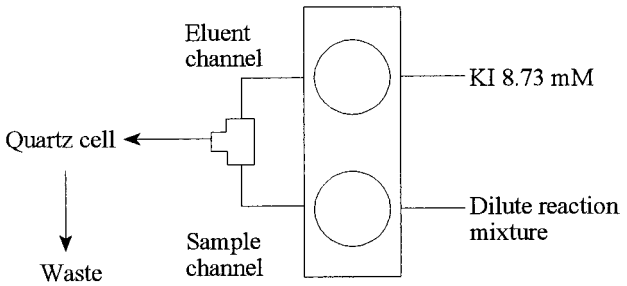

Figure 3. Spectroiodometric flow system.

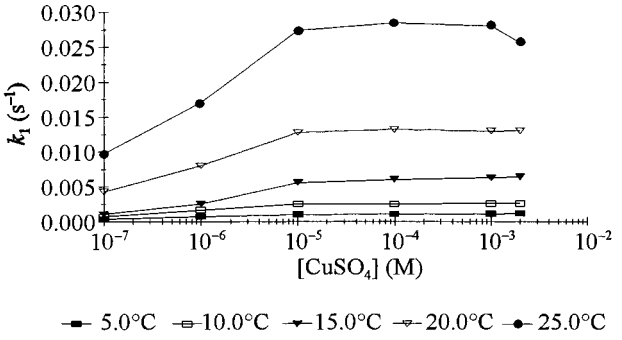

Figure 4. Impact of Cu^{2+} on the observed first-order decay rate constant of $HOONO_2$ at room temperature in 23 mM HNO_3.

Flow spectroiodometric runs lasted 4 min, with 1 s long readings taken every 5 s. The reaction vessel was first filled with 50 mL of the appropriate HNO_3 or buffer solution, and then a reaction mixture aliquot (20.0−100 μL) was added. Normally, the pump was started at 50 rpm shortly before the reaction mixture dilution (<10 s) to start flushing the cell of the previous run's solution, to eliminate the air in the tube, and also to get the dilute reaction mixture to the cell as soon as possible after dilution. Then the pump speed was reduced back to 25 rpm and the spectrophotometer started (8−20 s after dilution). The withdrawal of some of the solution before adding the reaction mixture introduces a slight error in the $HOONO_2$ concentration, but does not affect the pseudo-first-order decays studied.

Results and Discussion

Copper-Catalyzed Decay of $HOONO_2$. It has been reported that Cu(II) catalyzes a vigorous decomposition of $HOONO_2$.[5] We confirmed this using flow spectroiodometry by adding $CuSO_4$ without Na_2EDTA to the dilute reaction mixture. At higher $CuSO_4$ concentrations, the catalytic effect reached a plateau, as illustrated by Figure 4. This is consistent with the catalysis being due to reactions 1−2 and 9−10,[12] with the forward reaction 1 becoming the rate-limiting step at higher $CuSO_4$ concentrations.

$$HO_2 + Cu^{2+} \rightarrow H^+ + O_2 + Cu^+ \quad (9)$$

$$HO_2 + Cu^+ + H^+ \rightarrow H_2O_2 + Cu^{2+} \quad (10)$$

The temperature dependence of k_1, the rate constant of reaction 1, was studied between 5.0 and 25.0 °C with $CuSO_4$ concentrations varying between 0.1 and 2000 μM in dilute reaction mixtures prepared from 0.10 M chloroacetate buffer set at pH 3.01 ± 0.01. This pH was used to prevent regeneration of $HOONO_2$ as discussed below. At 10 μM Cu^{2+} and above, decay rate constants at a given temperature were almost independent of $[Cu^{2+}]$; they can be found in Table 1. The temperature dependence is shown in Figure 5; fitting to the

TABLE 1: Measured Values of k_1 at pH 3.01 ± 0.01[a]

temp (°C)	k_1 (10^{-3} s^{-1})
5.0	1.09 ± 0.10
10.0	2.51 ± 0.08
15.0	5.9 ± 0.6
20.0	12.5 ± 0.3
25.0	26 ± 2

[a] Averages of measurements for $[CuSO_4] \geq 10^{-5}$ M ($n = 4$). Numbers corrected for contribution of reaction 17.

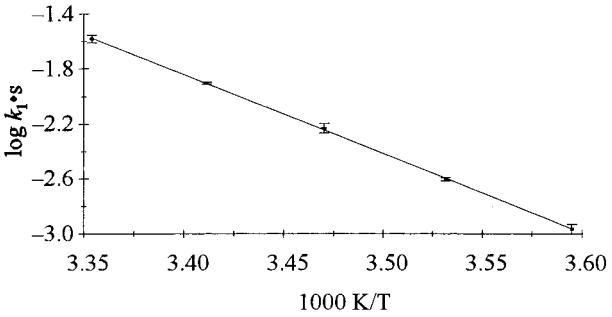

Figure 5. Arrhenius plot for $HOONO_2 \rightarrow HO_2 + NO_2$ (k_1). Solid line obtained by linear regression.

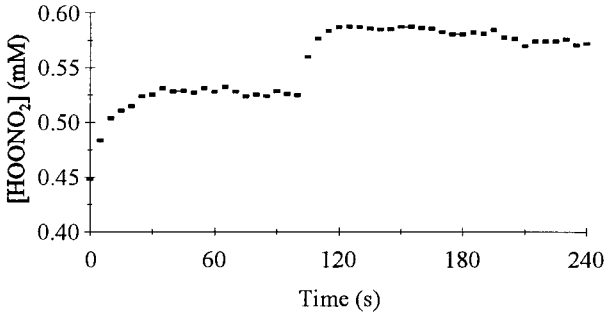

Figure 6. Impact of the addition of 0.03 mmol of $NaNO_2$ to 50 mL of dilute reaction mixture at pH 1.75. 46 ± 2 mmol H_2O_2 in solution before addition.

Arrenhius equation gives $k_1 = (5.27 \pm 0.15) \times 10^{17}$ s^{-1} exp(−110.1 ± 1.3 kJ mol^{-1}/(RT)). This large pre-exponential factor implies that the rate-limiting step is not a simple bond scission. At lower pH, a stronger temperature dependence was observed. The error limits given here only represent random, nonsystematic errors.

At 25.0 °C we found $k_1 = (2.6 \pm 0.2) \times 10^{-2}$ s^{-1}. Løgager and Sehested[4] measured $k_{-1} = (1.8 \pm 0.2) \times 10^9$ M^{-1} s^{-1}. Combining these gives the equilibrium constant, $K_1 = (1.5 \pm 0.2) \times 10^{-11}$ M.

The $HOONO_2$ lifetime in absence of catalyst can be evaluated by applying the steady-state approximation to reactions 1−3; this gives eq IV, where τ is the observed $HOONO_2$ lifetime. k_2

$$1/\tau = 2K_1\sqrt{k_2 k_3} \qquad \text{(IV)}$$

is reported to be $(9.0 \pm 0.7) \times 10^5$ M^{-1} s^{-1}.[13,15] Reported values of k_3 range from 1.5×10^7 to 1.0×10^8 M^{-1} s^{-1};[14] we used $(6.5 \pm 3.5) \times 10^7$ M^{-1} s^{-1}. At 25 °C, this yields $\tau = 78 \pm 13$ min.

Regeneration of $HOONO_2$. Experiments of the same kind at a lower pH (1.7−1.8) gave a much larger pre-exponential factor and activation energy. We believe that this was due to $HOONO_2$ regeneration which could be demonstrated as follows. Small aliquots of $NaNO_2$ solution were added to dilute reaction mixtures at pH 1.8 and 3.0 in the middle of flow spectroiodometric runs. This caused a sudden absorbance increase at the lower pH value, but not at the higher one; this is shown in Figure 6. This implies that $HOONO_2$ is regenerated, probably through reactions 3, 11, and 12. The enhanced temperature dependence

TABLE 2: Impact of Na_2EDTA on $HOONO_2$ Lifetimes

[Na_2EDTA] (mM)	lifetimes (s) avg	st dev	min	max	n
0	1340	940	350 ± 60	2240 ± 60	5
1.00	2860	1060	230 ± 40	4220 ± 110	25

TABLE 3: Comparison of Measured $HOONO_2$ Lifetimes

T (K)	τ (s)	reference
284	640	Kenley et al.[2]
293	8300	Kenley et al.[2]*
298	1000	Lammel et al.[3]
298	1400	Løgager and Sehested[4]
298	2600	Appelman and Gosztola[5] [a]
295	3000	this work, direct
298	6500	this work, indirect

[a] Undiluted reactions mixtures, presumably ≈ 1 M $HOONO_2$; all others being more dilute, probably in the 10^{-3} M $NOONO_2$ range.

$$H_2O_2 + HNO_2 \rightarrow HOONO + H_2O \qquad (11)$$

$$H_2O_2 + HOONO \rightarrow H_2O + HOONO_2 \qquad (12)$$

at low pH indicates that the regeneration was favored at low temperature. Conditions were such that no N(III) could have survived long enough to oxidize I^-. Given the rate constant of 1 s^{-1} for HOONO isomerization to nitric acid,[15] we had initially thought that all the HNO_2 produced or added to the system would end up as NO_3^- due to its fast reaction with the relatively large concentrations of H_2O_2. Apparently, this is not the case at low pH. Two acid-catalyzed reactions are involved: formation of HOONO and formation of $HOONO_2$. The first one proceeds via reactions 13 and 14,[16] and we propose reactions 15 and 16 for the second one. One of the pathways suggested

$$HNO_2 + H^+ \rightleftharpoons H_2O + NO^+ \qquad (13)$$

$$NO^+ + H_2O_2 \rightarrow HOONO + H^+ \qquad (14)$$

$$HOONO + H^+ \rightleftharpoons H_2O + NO_2^+ \qquad (15)$$

$$NO_2^+ + H_2O_2 \rightarrow HOONO_2 + H^+ \qquad (16)$$

by Appelman and Gosztola for the synthesis of $HOONO_2$ involves HOONO dissociation into OH and NO_2, but the most recent research on HOONO rejects this theory.[17] Moreover, all the other known syntheses of $HOONO_2$(aq) seem to involve NO_2^+ at one point or another.[2] The highly acidic conditions required for the synthesis of $HOONO_2$ are consistent with the mechanism proposed here. HOONO isomerization is known to be enhanced at pH below 2.[18]

Thermal Decay of $HOONO_2$. Using classical spectroiodometry, we found that the first-order $HOONO_2$ decay rates at room temperature (22 ± 1 °C) in 0.02 M HNO_3 were highly variable. Addition of 1.00 mM Na_2EDTA to the dilute reaction mixture lengthened lifetimes, as shown in Table 2. We attribute this high variability to impurities, most likely transition metals, perhaps including, but not limited to, Cu(II). We believe that the shorter lifetimes previously reported (see Table 3) are due to such impurities. Nevertheless, Na_2EDTA did not reduce the standard deviation of the lifetime distribution, contrary to what one might expect. The principal reason probably is the fact that these measurements were done over a period of several

months, which might introduce a lot of variability in the source, nature, and amount of trace contaminants. Furthermore, the low pH could have had a significant impact on what metal ions would be efficiently complexed by the chelating agent. It appears that under some conditions, Na_2EDTA was not effective at reducing the effect of the trace contaminants.

When the solutions contained Na_2EDTA, the lifetimes fell into two groups, with short lifetimes still occurring for a few runs. The 28 runs with lifetimes of more than 25 min gave an average of 49 ± 26 min. This is probably a lower limit, as much longer lifetimes were sometimes observed. The longest one was 73.9 ± 0.9 min in 0.019 M H_2SO_4. Even this is smaller than the lifetime of 111 ± 19 min expected from eq IV at room temperature; it would not be surprising to see longer lifetimes measured under similar conditions in the future, but with purer reactants. We do not believe this particularly slow decomposition to be due to the different acid, as other sets of runs in H_2SO_4 showed faster decays. At this pH though, the lifetime is likely to be extended by $HOONO_2$ regeneration; our own measurements suggest an effect of 8 ± 13%.

Stoichiometric Ratio. In the radical mechanism, reactions 1−3, $HOONO_2$ decay leads to the production of equal amounts of H_2O_2 and HNO_2. These will react together to make peroxynitrous acid, reaction 11, which should then very quickly isomerize to nitric acid.[18] Overall, one would observe a stoichiometric ratio, $d[H_2O_2]/d[HOONO_2]$, of 0 if there is no regeneration of $HOONO_2$.

Løgager and Sehested[4] report a stoichiometric ratio of unity in solutions where concentrations were comparable to those in our dilute reaction mixtures. This H_2O_2 loss is consistent with reaction 4 as the low-pH decay mechanism, instead of the radical mechanism, reactions 1−3. On the other hand, Appelman and Gosztola found a stoichiometric ratio of 0.64 in undiluted reaction mixture.[5]

Classical spectroiodometry was used to determine the stoichiometric ratio, $S = d[H_2O_2]/d[HOONO_2]$. In 24 mM HNO_3, pH 1.7−1.8, where decay through NO_4^- should be negligible, a significant Na_2EDTA impact was found. In five runs without Na_2EDTA, the average ratio was 0.25 ± 0.18, while in 25 runs with 1.00 mM Na_2EDTA, the average was 0.03 ± 0.07. The ranges were 0.00 to 0.381 and −0.31 to 0.35, respectively. Combining all the data, we found that $S = 0.29 \pm 0.30 - ((8.3 \pm 4.8) \times 10^{-5}\ \mathrm{sec}^{-1})\tau$, where τ is the $HOONO_2$ lifetime. The intercept of this equation is the stoichiometric ratio when the catalyzed decay dominates. S is near 0 for lifetimes of about 1 h and, presumably, longer. The squared correlation coefficient, R^2, of 0.288 implies a significant correlation at the 99% level.

These results imply that $HOONO_2$ decays through reactions 1−3 and 11, contrary to what Løgager and Sehested concluded.[4] The high susceptibility of $HOONO_2$ decay to catalysis by impurities is likely to have affected their results. One of our own experiments showed that addition of $CuSO_4$ to a dilute reaction mixture in the middle of a set of classical spectroiodometric measurements caused not only a substantial loss in $HOONO_2$ but also in H_2O_2, as shown in Figure 7. Also, if there is regeneration of $HOONO_2$, a stoichiometric ratio somewhat above 0 is expected since each HNO_2 molecule that eventually ends back again as $HOONO_2$ would consume two H_2O_2 molecules. This would be particularly true in the undiluted reaction mixtures studied by Appelman and Gosztola.[5]

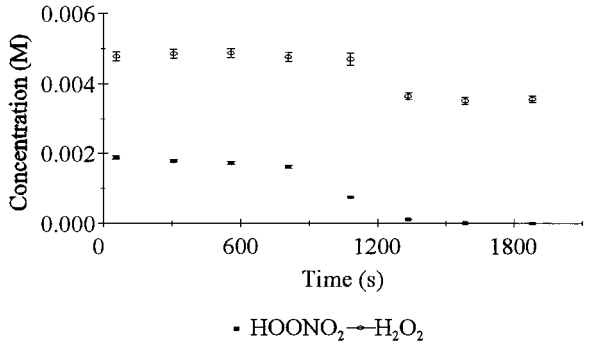

Figure 7. Impact of the addition of 97.2 nmol of $CuSO_4$ to 50 mL of dilute reaction mixture.

Løgager and Sehested determined the stoichiometric ratio by adding HNO_2 to their reaction mixture and using the initial rapid change in HNO_2 absorbance to determine $[H_2O_2]$. A subsequent slower change was used to measure $[HOONO_2]$. However, they could only measure the decay of HNO_2 due to reaction with $HOONO_2$ beginning 10−20 s after addition. Given their reported concentrations and rate constants, 40−60% of the $HOONO_2$ would have reacted during mixing. This implies that much, if not all, of their measured change in $[H_2O_2]$ was really due to the change in $[HOONO_2]$. Furthermore, they assume a stoichiometry of $d[HNO_2]/d[HOONO_2] = 1$, which is less than sure, as will be shown later. Finally, they do not give any indication of the reproducibility or the uncertainty in their stoichiometric ratio. Their results do agree with ours in implying that any loss of H_2O_2 must be due to reaction with the $HOONO_2$ decomposition products since H_2O_2 is stable once $HOONO_2$ is gone.

$HOONO_2$(aq) Thermodynamics. With the measured value of K_1, we get $\Delta G_1^\circ = 61.8 \pm 0.3$ kJ mol^{-1}. Using the standard Gibbs energies of formation for HO_2(aq) and NO_2(aq) given in Table 4, we obtain $\Delta G^\circ_{f,298}(HOONO_2(aq)) = 5.5 \pm 1.5$ kJ mol^{-1}.

$S^\circ_{298}(HOONO_2(g))$ was calculated using statistical thermodynamics[19] using the $HOONO_2$ molecular structure calculated by Saxon and Liu with basis set SCF-6-31G.[20] The vibrational contribution was calculated based on the data reported by Friedl et al.[21] Two bands have not been observed in the gas phase yet, but estimates have been made for them.[22,23]

The entropies associated with the HO−ONO_2 and HO_2−NO_2 torsional motions may be substantially modified by internal rotation. The rotational barriers are unknown, but those of the analog molecule CH_3ONO_2 have been measured.[24] Using the treatment of Pitzer[25] with the peroxynitric acid rotors' reduced moments of inertia, we estimated barriers of 9.6 and 38 kJ mol^{-1}, respectively. We deemed the second one too high for

TABLE 4: Thermochemical Properties Used in Calculations[a]

	$HOONO_2$	HO_2	NO_2	H_2O_2	HNO_2
$\Delta G^\circ_{f,298}$(aq) (kJ mol^{-1})	[5.5 ± 1.5]	5.1 ± 0.8[30]	[62.2 ± 1.2]	−134.1[31]	−50.6[34]
S°_{298}(g) (J K^{-1} mol^{-1})	[294 ± 3]	229.11 ± 0.08[32]	240.034 ± 0.13[35]	232.991[35]	254[34]
$\Delta S^\circ_{solv,298}$ (J K^{-1} mol^{-1})	[−113 ± 4]	[−92 ± 8]	[−113 ± 4]	−100[29]	−104[33]
H_{298} (M atm^{-1})	[12700 ± 4700]	[5760 ± 500][33]	0.012 ± 0.004[34]	83300 ± 3800[35]	49 ± 3[36]

[a] Values calculated or evaluated in this paper are between brackets. The Henry's Law constant for HO_2 is based on the calculation of Schwartz[33] but using the thermodynamics for HO_2(g) determined from the equilibrium constant measured by Hills and Howard[36] together with data for ClO from Abramowitz and Chase.[37]

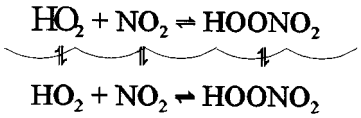

Figure 8. Cycle used for the calculation of the Henry's Law constant of $HOONO_2$.

rotation to be significant in comparison to the corresponding torsional vibration. Depending on which wavenumber estimates were used for the yet-undetected bands and whether the HO−ONO_2 torsion was treated as a vibration or a hindered rotation, the gas-phase standard entropy varied between 290.3 and 297.0 J K^{-1} mol^{-1}. For the following calculations, we used an average value of 294 ± 3 J K^{-1} mol^{-1}. By comparison, Chen and Hamilton have computed 297 J K^{-1} mol^{-1} from ab initio calculations.[26]

The method of Berdnikov and Bazhin[26] was used to estimate the standard solvation entropies, $\Delta S°_{solv,298}$, for HO_2, NO_2 and $HOONO_2$ (cf. Table 4). Using these, we approximate $S°_{298}(HOONO_2(aq))$ to be 181 ± 5 J K^{-1} mol^{-1}.

From K_1 and the standard entropies, the standard enthalpy of reaction 1 at 298 K is found to be 87 ± 3 kJ mol^{-1}. From the standard Gibbs energy of formation and standard entropy for $HOONO_2(aq)$, together with the entropies of the elements,[35] we obtain $\Delta H°_{f,298}(HOONO_2(aq)) = -111.0 \pm 2.0$ kJ mol^{-1}.

From the enthalpy and activation energy of reaction 1, we obtain an activation energy of 23 ± 3 kJ mol^{-1} for the reverse reaction. This is somewhat higher than the value of 18 kJ mol^{-1} expected for a diffusion-limited reaction over this temperature range. We expect the activation energy for the association reaction (k_{-1}) to be smaller than that for a diffusion-limited reaction. This is because the rate constant (1.8×10^9 M^{-1} s^{-1}) is smaller than expected for a diffusion-limited reaction and is close to that reported for the gas-phase reaction (2.8×10^9 M^{-1} s^{-1}). The gas-phase rate constant is nearly independent of temperature.[27]

Using the thermochemical cycle illustrated by Figure 8, the Henry's law constant for $HOONO_2$ was found to be 12600 ± 4700 M atm^{-1}, based on the Henry's law constants given in Table 4 and the values of K_1 in both the aqueous phase ($1.5 \pm 0.2 \times 10^{-11}$ M) and the gas phase ($1.12 \pm 0.06 \times 10^{-10}$ M).[28] From this and $\Delta S°_{solv,298}(HOONO_2)$, we find $\Delta H°_{solv,298}(HOONO_2) = -57.1 \pm 1.5$ kJ mol^{-1}. Combining that with $\Delta H°_{f,298}(HOONO_2(aq))$ leads to $\Delta H°_{f,298}(HOONO_2(g)) = -53.09 \pm 2.5$ kJ mol^{-1}. It is interesting to note that this Henry's law constant is intermediate between those of analog compounds H_2O_2 and HNO_2.

Finally, we calculated the reduction potential of $HOONO_2$ using the cycle shown in Scheme 1.

SCHEME 1

$$HOONO_2 + H_2 \rightarrow H_2O + H^+ + NO_3^-$$
$$\Delta G°_{298}\ (\text{kJ mol}^{-1}) = -354 \pm 2$$

$$H_2O \rightarrow H^+ + OH^- \qquad \Delta G°_{298}\ (\text{kJ mol}^{-1}) = 79.89$$

$$2\,H^+ + 2\,e^- \rightarrow H_2 \qquad \Delta G°_{298}\ (\text{kJ mol}^{-1}) = 0.00$$

$$HOONO_2 + 2\,e^- \rightarrow OH^- + NO_3^-$$
$$\Delta G°_{298}\ (\text{kJ mol}^{-1}) = -274 \pm 2$$

$$\Rightarrow \quad E° = 1.42 \pm 0.01\ \text{V}$$

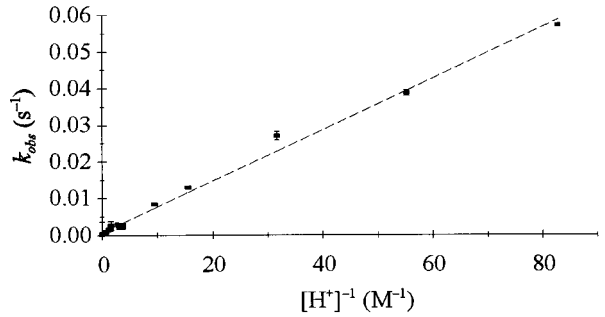

Figure 9. Effect of $[H^+]^{-1}$ on the $HOONO_2$ pseudo-first-order decay rate constant at room temperature. Line obtained by linear regression.

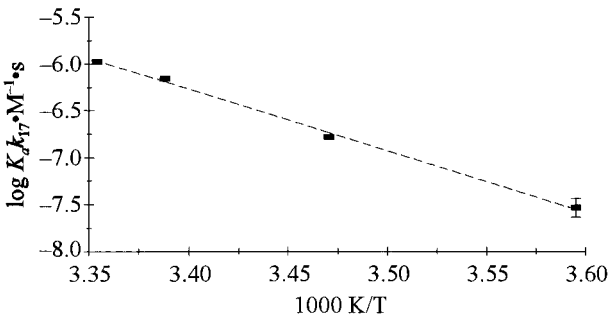

Figure 10. Arrhenius plot for $K_a k_{17}$. Line obtained by linear regression.

Decay at Moderate pH and Determination of $K_a k_{17}$. The observed stoichiometry for the basic decay of $HOONO_2$ is given by reaction 17.

$$NO_4^- \rightarrow NO_2^- + O_2 \qquad (17)$$

The pseudo-first-order decay rate constant of $HOONO_2$ was determined as a function of pH, using classical spectroiodometry. Figure 9 shows the expected linear behavior in $[H^+]^{-1}$ due to acid dissociation and reaction 17. From the slope we obtain the product $K_a k_{17} = (6.95 \pm 0.08) \times 10^{-7}$ M s^{-1} at room temperature for pH values between 1.66 and 4.92. At 25.0 °C, we observed, between pH 3.31 and 5.02, a product of 1.059 ± 0.014) × 10^{-6} s^{-1}. Using the pK_a of 5.85 ± 0.10,[4] this yields $k_{17} = 0.75 \pm 0.17$ s^{-1}, in reasonable agreement with the value of 1.0 ± 0.2 s^{-1} reported by Løgager and Sehested.[4]

The same experiment was repeated at 5.0 and 15.0 °C, in the pH range 3.3−5.0, and the results were combined with the previous ones to give an Arrhenius plot, Figure 10. This gave $K_a k_{17} = (1.16 \pm 0.20) \times 10^{16}$ M s^{-1} exp(−126 ± 8 kJ mol^{-1}/*RT*). Assuming that $HOONO_2$ has a typical entropy of ionization of −92 J K^{-1} mol^{-1},[29] we can use the pK_a at 25 °C to estimate the heat of ionization. This yields $K_a = 1.5 \times 10^{-5}$ M exp(−6 kJ mol^{-1}/*RT*) and $k_{17} = 7.7 \times 10^{20}$ s^{-1} exp(−120 kJ mol^{-1}/*RT*). This pre-exponential factor is unreasonably large for an elementary reaction.

Previous workers agree that the final products of NO_4^- decay are NO_2^- and O_2.[2−5] Nevertheless, this does not say anything about the mechanism, which might be more complex than the direct reaction implied by the stoichiometry.

It is interesting to compare k_{17} to the rate constant of reaction 18. From K_1 and the pK_a values of $HOONO_2$ and HO_2,[4,15] we

$$NO_4^- \rightleftharpoons NO_2 + O_2^- \qquad (18)$$

can estimate K_{18} to be (1.7 ± 0.3) × 10^{-10} M at 25 °C. Løgager and Sehested report that k_{-18} is (4.5 ± 1.0) × 10^9 M^{-1} s^{-1}.[4] Combining these, we find $k_{18} = 0.76 \pm 0.25$ s^{-1}, virtually identical to the value of k_{17} determined above. This may be a coincidence or it may be an indication that radical dissociation

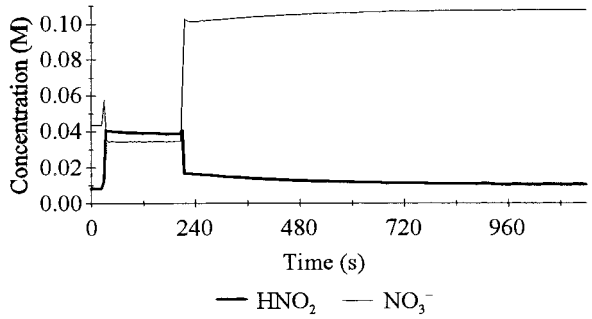

Figure 11. Addition of dilute reaction mixture to a HNO_2 solution. The first sharp change is acidification with HNO_3 of a $NaNO_2$ solution, and the second one, addition of the dilute reaction mixture. The slow change afterward is reaction between HNO_2 and $HOONO_2$.

is the first step in the high-pH decay and is followed by further radical reactions that lead to the final products. Thus, at room temperature, reaction 18 could be the rate-limiting step.

Another indication of the complexity of this chemistry is given by the reaction with HNO_2. Løgager and Sehested[4] measured the reaction rate of $HOONO_2$ with HNO_2 by stopped-flow spectrophotometry and found a rate constant of 12 ± 2 M^{-1} s^{-1} for reaction 19.

$$HOONO_2 + HNO_2 \rightarrow 2H^+ + 2NO_3^- \qquad (19)$$

We found that direct addition of dilute reaction mixture to excess HNO_2 in the stirred spectrophotometer cell at pH < 1 caused a very abrupt fall in HNO_2 concentration and an increase in the NO_3^- concentration, as observed spectrophotometrically. Surprisingly, the data presented in Figure 11 does not match the expected stoichiometry of -2 for reaction 19. Instead, plots of $[NO_3^-]$ against $[HNO_2]$ give an average slope of -0.90 ± 0.04, based on four replicate runs. This implies a nitrogen deficit. NO is the most likely suspect to account for this missing nitrogen. Furthermore, since it was impossible for us to quantify $HOONO_2$ and HNO_2 simultaneously, we cannot pronounce ourselves on the validity of Løgager and Sehested's assumption that $d[HOONO_2]/d[HNO_2] = 1$.

Conclusion

We have determined that in acidic solution, $HOONO_2$ decays *via* dissociation to free radicals followed by disproportionation of these radicals. By combining the rate constant for this reaction with the one reported for the reverse reaction, we have evaluated the thermodynamics of $HOONO_2$(aq). We find that the bond enthalpy is 87 ± 3 kJ mol^{-1} and that the activation energy for the dissociation reaction is 110 ± 1 kJ mol^{-1}. The latter's uncertainty only accounts for the effect of random statistical errors. Since it is based on measurements over a narrow temperature range, the value will be sensitive to small systematic errors. It is likely that the activation energy is somewhat too large, since it leads to an unreasonably large activation energy of 23 ± 3 kJ mol^{-1} for the reverse reaction.

On the other hand, the bond enthalpy is not subject to this problem. It is not based on a van't Hoff plot but rather on equilibrium data at a single temperature, absolute entropies, and auxiliary thermodynamic data for HO_2 and NO_2. Here, the main source of uncertainty is the estimated solvation entropy for HO_2. Thus, the uncertainty given here should be a reasonable estimate of both random and systematic errors.

The decay in acidic solution is catalyzed by trace metal ions. As a result, small amounts of contaminants make it difficult to directly measure the true value of the thermal decay rate constant. From the dissociation equilibrium constant and the reported rate constants for the NO_2 and HO_2 disproportionation reactions, we calculate a lifetime of 78 ± 13 min toward thermal decay at 25 °C.

Our results for the base-catalyzed decay agree with those previously reported by Løgager and Sehested. However, the very high activation energy (120 kJ mol^{-1}) and pre-exponential factor (7.7×10^{20} s^{-1}) imply that this may not proceed via an elementary reaction that produces O_2 directly. The decay may proceed via dissociation to the radicals followed by some as yet unidentified reaction of the radicals.

The solubility of $HOONO_2$ is critical to evaluating its effect on the chemistry of atmospheric particles. We have determined that the Henry's Law constant for $HOONO_2$ at 298 K is $(13 \pm 5) \times 10^3$ M atm^{-1} and that the heat of solvation is -57.1 ± 1.5 kJ mol^{-1}. The importance of this high solubility for aqueous-phase chemistry in the atmosphere can be illustrated by comparison with O_3. O_3 is one of the most important atmospheric oxidants in both the gas and aqueous phases. Under moderately clean conditions, one might expect to find a mixing ratio of 30 ppbv for O_3 4 orders of magnitude greater than the 2.4 pptv expected for $HOONO_2$ (in equilibrium with 30 pptv of HO_2 and 60 pptv of NO_2) at a typical temperature of 288 K. However, the corresponding equilibrium aqueous-phase concentration of $HOONO_2$ is 6×10^{-8} M, a factor of 100 larger than for O_3(aq) (5×10^{-10} M). Thus, $HOONO_2$ may play a much more important role in atmospheric droplets than would be expected from its very small gas-phase concentration.

Acknowledgment. We thank Dr. Tim Johnson for his help in trying to synthesize $HOONO_2$ and in quantifying it spectrophotometrically, Dr. E. H. Appelman for advice on the synthesis and iodometry, Bruker Spectrospin Canada for use of their FT-Raman spectrophotometer, the Ontario Laser and Lightwave Research Centre for use of their Raman spectrophotometer. This work was supported by the Natural Sciences and Engineering Research Council of Canada.

References and Notes

(1) Baldwin, A. C.; Barker, J. R.; Golden, D. M.; Hendry, D. G. *J. Phys. Chem.* **1977**, *81*, 2483.
(2) Kenley, R. A.; Trevor, P. L.; Lan, B. Y. *J. Am. Chem. Soc.* **1981**, *103*, 2203.
(3) Lammel, G.; Perner, D.; Warneck, P. *J. Phys. Chem.* **1990**, *94*, 6141.
(4) Løgager, T.; Sehested, K. *J. Phys. Chem.* **1993**, *97*, 10047.
(5) Appelman, E. H.; Gosztola, D. J. *Inorg. Chem.* **1995**, *34*, 787.
(6) Eriksson, E. *Tellus* **1960**, *12*, 63.
(7) Keene, W. C.; Pszenny, A. A. P.; Jacob, D. J.; Duce, R. A.; Galloway, J. N.; Schultz-Tokos, J. J.; Sievering, H.; Boatman, J. F. *Global Biogeochem. Cycles* **1990**, *4*, 407.
(8) Pszenny, A. A. P.; Keene, W. C.; Jacob, D. J.; Fan, S.; Maben, J. R.; Zetwo, M. P.; Springer-Young, M.; Galloway, J. N. *Geophys. Res. Lett.* **1993**, *20*, 699.
(9) Jobson, B. T.; Niki, H.; Yokouchi, Y.; Bottenheim, J.; Hopper, F.; Leaitch, R. *J. Geophys. Res.* **1994**, *99*, 25355.
(10) Ramette, R. W.; Sandford, R. W., Jr. *J. Am. Chem. Soc.* **1965**, *87*, 5001.
(11) Awtrey, A. D.; Connick, R. E. *J. Am. Chem. Soc.* **1951**, *73*, 1842.
(12) Bielski, B. H. J.; Cabelli, D. E.; Arudi, R. L. *J. Phys. Chem. Ref. Data* **1985**, *14*, 1041.
(13) Christensen, H.; Sehested, K. *J. Phys. Chem.* **1988**, *92*, 3007.
(14) Neta, P.; Huie, R. E.; Ross, A. B. *J. Phys. Chem. Ref. Data* **1988**, *17*, 1027.
(15) Brice, K. A.; Penkett, S. A. Report No. AERE-R9260; Atomic Energy Research Est.: Harwell, England, 1978.
(16) Anbar, M.; Taube, H. *J. Am. Chem. Soc.* **1954**, *76*, 6243.
(17) Koppenol, W. H.; Moreno, J. J.; Pryor, W. A.; Ischiropoulos, H.; Beckman, J. S. *Chem. Res. Toxicol.* **1992**, *5*, 834.
(18) Edwards, J. O.; Plumb, R. C. *Progress in Inorganic Chemistry*; Karlin, K. D., Ed.; John Wiley & Sons: New York, **1994**; Vol. 41, pp 599.
(19) Benson, S. W. *Thermochemical Kinetics*, 2nd ed.; John Wiley & Sons: New York, **1976**; Chapter 2.
(20) Saxon, R. P.; Liu, B. *J. Phys. Chem.* **1985**, *89*, 1227.

(21) Friedl, R. R.; May, R. D.; Duxbury, G. *J. Mol. Spectrosc.* **1994**, *165*, 481.
(22) Baldwin, C.; Golden, D. M., Jr. *J. Phys. Chem.* **1978**, *82*, 644.
(23) Chen, Z.; Hamilton, T. P. *J. Phys. Chem.* **1996**, *100*, 15, 731.
(24) Dixon, W. B.; Wilson, E. B., Jr. *J. Chem. Phys.* **1961**, *35*, 191.
(25) Lewis, G. N.; Randall, M.; Pitzer, K. S.; Brewer, L. *Thermodynamics*, 2nd ed.; McGraw-Hill: New York, 1961; Chapter 27.
(26) Berdnikov, V. M.; Bazhin, N. M. *Russ. J. Phys. Chem.* **1970**, *44*, 395.
(27) Zabel, F. *Z. Phys. Chem. (Munich)* **1995**, *188*, 119.
(28) DeMore, W. B.; Sander, S. P.; Golden, D. M.; Hampson, R. F.; Kurylo, M. J.; Howard, C. J.; Ravishankara, A. R.; Kolb, C. E.; Molina, M. J. *Chemical Kinetics and Photochemical Data for Use in Stratospheric Modeling*, JPL publ. 92-20, Jet Propulsion Laboratory: Pasadena, CA, 1992.
(29) Pitzer, K. S. *J. Amer. Chem. Soc.* **1937**, *59*, 2365.
(30) Schwartz, S. E. *J. Geophys. Res.* **1984**, *89*, 11, 589.
(31) Weast, R. C. Selected Values of Chemical Thermodynamic Properties. *Handbook of Chemistry and Physics*, 1st student ed.; CRC Press, Inc.: Boca Raton, FL, 1987.
(32) Chase, M. W., Jr.; Davies, C. A.; Downey, J. R., Jr.; Frurip, D. J.; McDonald, R. A.; Syverud, A. N. *JANAF Thermochemical Tables*, 3rd ed.; American Institute of Physics: New York, 1986.
(33) Park, J.-Y.; Lee, Y.-N. *J. Phys. Chem.* **1988**, *92*, 6294.
(34) Schwartz, S. E.; White, W. H. *Advances in Environmental Science and Engineering*; Pfafflin, J. R., Ziegler, E. N., Eds.; Gordon and Breach: New York, 1981; pp 1.
(35) O'Sullivan, D. W.; Lee, M.; Noone, B. C.; Heikes, B. G. *J. Phys. Chem.* **1996**, *100*, 3241.
(36) Hills, A. J.; Howard, C. J. *J. Chem. Phys.* **1984**, *81*, 4458.
(37) Abramowitz, S.; Chase, M. W. *Pure Appl. Chem.* **1991**, *63*, 1449.